Achieving Motion in a Plane Orthogonal to the Substrate

Mohan Vamsi Dunga
Srinath Satyanarayana
University of California, Berkeley, CA 94704.

Introduction

Recent developments in silicon-based fabrication technology such as fusion bonding, deep reactive ion etching (DRIE) [1] and polyamide joints [2] are expected to enable batch fabrication of mechanically robust micromechanisms that are capable of true 3-D motion. Several MEMS structures and mechanisms have been made for motion in a plane parallel to the surface as in the case of accelerometers (ADXL50) or for out of plane motion as in the case of beam steering using mirrors. However, 3-D motion has not been achieved in the complete sense as not much work has been done in the area of rotary/linear motion in a plane orthogonal to the substrate. In this paper a mechanism for generating rotary motion in a plane perpendicular to the substrate is proposed. This concept can be used to achieve both rotary and linear motion in the orthogonal plane. The key issue for achieving motion in an orthogonal plane lies in the coupling between the mechanisms on the substrate to the mechanisms in the orthogonal plane. A mechanical coupling similar to the bevel gear system is used for transmitting motion/power to the mechanisms in the orthogonal plane.

Conceptual Design

The central part of the proposed mechanism for achieving rotary motion in an orthogonal plane consists of two gears, one in each of the two perpendicular planes. In the macro scale this can be done using a bevel gear system as shown in Fig.1. Bevel gears are difficult to fabricate in MEMS so a different gear mechanism is proposed. A schematic of the proposed mechanism is shown in Fig.2 in which the horizontal gear (G2) drives the vertical gear (G1). The two side plates are used to keep G1 perpendicular to G2.

Figure 1 Bevel gear mechanism.
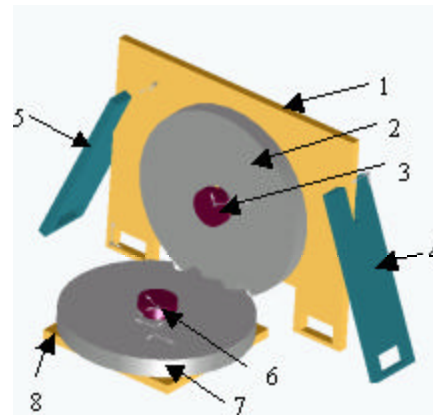
1 – Base plate (G1)	5 – Side plate #2
2 – Gear 1 (G1)	6 – G2 Pin
3 – G1 Pin	7 – Gear 2 (G2)
4 – Side plate #1	8 – Base plate (G1)

Figure 2 Proposed mechanism for achieving motion in a orthogonal plane.

Design Calculations

The proposed mechanism will be fabricated using SUMMiT V process developed by SANDIA. The critical parameters are designed based on the process design rules. The parameters and critical dimensions are shown in Fig.3. The design process for a mechanism having G2 with radius 100 μm and G1 with radius 50 μm (a transmission ratio of 2) has been shown as an example. Since the gears are fabricated in Poly3 layer, their thicknesses are fixed at 2.25 μm.
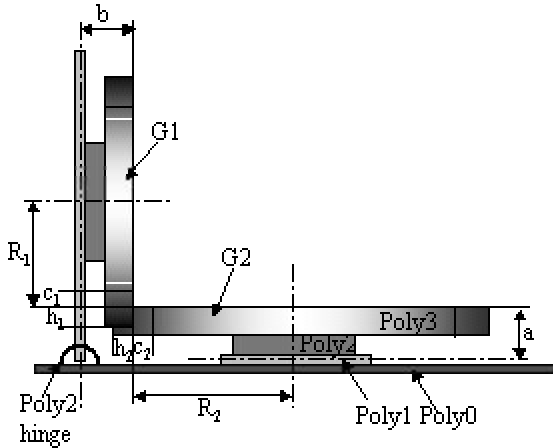
Figure 3 Design parameters for the mechanism.

The most crucial parameter is "h" as it decides the interlocking between the gears and if they can rotate without crashing. When G1 rotates by one tooth angle (θ), the tooth of G1 should clear the plane in which the G2 lies (Fig. 4). This imposes the constraint that one tooth angle movement corresponds to a vertical displacement of "h" which should be greater than the thickness of G2 (t) which is 2.25 μm (Eqn. 1).
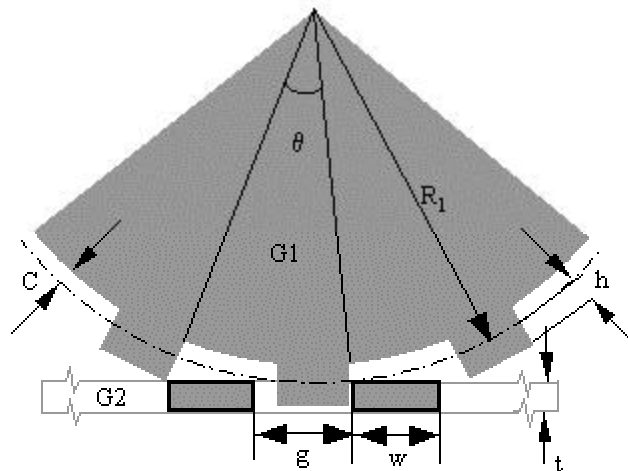

Figure 4 Constraint on gear interlocking.

$$R_1(1-\cos q)/\cos q = h > t; q = 2p/N_1 \quad (1)$$

As G2 has a vertical play of ± 0.15 μm due to pin joint in Poly1, the constraint is changed to $h > t + 0.15$ μm. Taking process variations into account, "h" for G1 was chosen

to be 2.5 μm. The above constraint gives the freedom to choose any "h" for G2. To keep symmetry in the structure, "h" for G2 was also chosen to be 2.5 μm. Using the constraint on G1 (Eqn. 1), the number of teeth (N_1) was calculated to be 20. For a transmission ratio of 2, the number of teeth of G2 (N_2) has to be 40. For proper interlocking, the teeth width (w) and the teeth spacing (g) for both gears have to be the same and "w" has to be less than "g"(Fig. 4). Simple geometry considerations give

$$w + g = 2pR_1/N_1 = 2pR_2/N_2 = 15.7\,mm \quad (2)$$

Using the above result, "w" and "g" were set to 7 μm and 8.7 μm, respectively, for both the gears. The gear teeth profile is made rectangular, as it is not possible for fabricating an involute profile along the layer thickness. In order to allow the gears to lock during assembly, a clearance "c" of 3 μm (Fig. 4) is used for both the gears.

The pin joint flange will most likely fail by shear because of its short height. The material shear strength thus sets a minimum radius requirement. The interaction force (F) between the two gear teeth is transmitted to the two gear hubs. Since this force (F) is also limited by the material shear strength, the minimum radius depends only on geometry (Eqn. 3).

$$r = \sqrt{wt/p} = 2.24\,mm \quad (3)$$

In order to make sure that the flange does not break r was chosen to be 4 μm. The gears are fabricated in the same plane and their center-to-center distance is governed by the dimensions "a" and "b" (Fig.3). To constrain the motion of G1 in vertical plane, the hinge thickness (W) is set equal to hinge gap (H) as shown in Fig.5. The final design parameters of the mechanism are summarized in Table 1.

Table 1 Design parameters for the mechanism.

R_1	50 μm	R_2	100 μm
N_1	20	N_2	40
w	7 μm	g	8.7 μm
h	2.5 μm	c	3 μm
r_1	6 μm	r_2	4 μm
R_{hub1}	20 μm	R_{hub2}	27 μm
a	6.55 μm	b	6.55 μm
H	3.5 μm	W	3.5 μm

Fabrication

The mechanism is fabricated using the Sandia SUMMiT V process, a 5-level MEMS technology, which uses traditional IC processing and has 4 Poly Si structural layers [3]-[4].

The base plate for G1 is made in Poly1, which is hinged to Poly0 by Poly2 and once flipped it is held in position by side flaps that are also made in Poly1 and hinged to Poly0 by Poly2. In order to minimize the contact area between the gears and the base plates a hub is used to separate them. The hub is made in Poly2 and is attached to Poly1 using unflanged pin joint. The base plate for G2 is made in Poly1 and is anchored to Poly0. The hub for G2 is made in Poly2 and is attached to Poly1 using a flanged pin joint. Both G1 and G2 are fabricated in Poly3. The structures are finally released using a wet etch. Cross sections of the two gears are shown in Fig. 5.
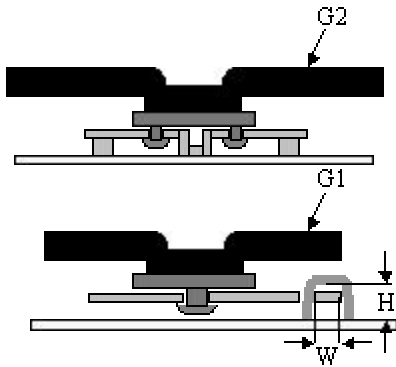

Figure 5 Gear cross sections.

Performance Analysis

The interaction force (F) between the gear teeth is equal to the ratio of transmitted torque and the gear radius. The force causes the teeth to shear and hence the maximum torque is limited by the yield stress (σ_y) of Poly Si and the gear teeth cross-section as shown in Eqn. 4, where, k (safety factor) is equal to 2.

$$T_{1\max} = (\sigma_y/2k)(w*t)*R_1$$
$$= (N_1/N_2)T_{2\max} \tag{4}$$

The maximum power transmitted is given by Eqn. 5.

$$P_{\max} = T_{1\max}w_1 = T_{2\max}w_2 \tag{5}$$

The efficiency of the system is affected by the frictional and damping losses. The frictional losses between the gear hub and base plate can be neglected, as the masses of the gears are very low. But there is sufficient friction between the hubs and pin-joints due to the gear teeth interaction force (F). For a friction coefficient μ, the friction torque (T_F) is given by Eqn. 6.

$$T_F = \mu F r \tag{6}$$

For a power input P_i to G2, the output power P_{O2}, which is also the power input to G1, is given by Eqn. 7.

$$P_{O2} = P_i(1 - \mu r_2/R_2) \tag{7}$$

The power transmitted by G1, which is the power output from the mechanism that can be used by any other device in the orthogonal plane, is given by Eqn. 8.

$$P_{Out} = P_{O2}(1 - \mu r_1/R_1)$$
$$= P_i(1 - \mu r_1/R_1)(1 - \mu r_2/R_2) \tag{8}$$

Couette damping is assumed to exist between the gear hub and the base plate and the damping power loss is given by Eqn. 9 (μ_v is the viscosity of air)

$$P_{damp} = \frac{p\mu_v}{2t_{sacox2}}(R_{hub1}^4 w_1^2 + R_{hub2}^4 w_2^2) \tag{9}$$

The total losses (P_{losses}) in the mechanism are given by sum of the frictional losses and damping losses. Hence the efficiency of the system is given by Eqn. 10.

$$\eta = (P_i - P_{losses})/P_i \tag{10}$$

An important phenomenon that affects structures in these dimensions is "stiction". There is no accurate estimate of stiction but it is proposed to measure it using one of the test structures. The performance parameters for the designed mechanism with G2 being driven at 1500 rpm are tabulated in Table2. μ was chosen to be 0.5 [5] and σ_y was chosen to be 1GPa [6]. From Table2, it is seen that P_{damp} is negligible compared to P_{fric}. So, the efficiency of the mechanism is determined by the friction losses, which is equal to 93%.

Table 2 Performance Parameters

F_{max}	3.94 mN	ω_1	3000 rpm
T_{1max}	0.20 μN-m	T_{2max}	0.40 μN-m
P_{max}	62.8 μW	P_{fric}	0.07 P_i
P_{damp}	2.72 pW	η	0.93

Test Structures

Test structures have been designed to validate the design. The test structures will be driven by SANDIA's microengine [6]-[7].

To test the gear ratio, N_2 is varied from 30 to 50 with N_l fixed at 20. The gear ratio is characterized by measuring the velocities of both gears with a CCD camera and a microscope.

Loss measurements are made by characterizing the frictional and damping losses separately. Frictional losses vary with pin joint radius (r), hence r_2 is varied from 4 µm to 20 µm in steps of 4 µm. As damping losses vary with hub radius (R_{hub}), R_{hub2} is varied from 20 µm to 40 µm in steps of 4 µm. If there is no load on G1, the power input to the mechanism is simply P_{loss}. Thus, by measuring the power input to the micro-engine the power losses can be estimated.

In order to find optimal "w" and "g" for smooth torque transmission, "w" is varied from 6 µm to 7.6 µm in steps of 0.2 µm while keeping w+g fixed and w<g. The transmission ratio (ω_2/ω_1) of the mechanism will be observed for each of the above test structures.

The threshold torque required to get the mechanism in motion determines the stiction in the system. This torque is measured by ramping the input torque until motion is observed. Alternately, it can also be measured using a linear rack and a force gauge (Fig. 6).
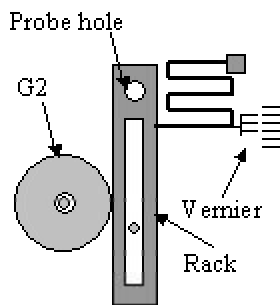

Figure 6 Setup for measuring stiction.

Expected Results

1. Figure 1: Transmission ratio vs. R_2 (test structure #1) – **Linear**.
2. Figure 2: P_{fric} vs. r_2 (test structure #2) – **Linear**. It can be used to characterize the friction coefficient.
3. Figure 3: P_{damp} vs. R_{hub2}^{4} – **Linear**.
4. Figure 4: Transmission ratio vs. w – A curve peaking at some intermediate value.

Conclusions

A novel mechanism for achieving motion in a plane orthogonal to the substrate was designed. The power transmission efficiency is very high and is limited only by coulomb friction. Fabrication of the mechanism in SUMMiT V gives it the flexibility to be interfaced with several existing MEMS devices. By using a linear rack, the rotational motion can be converted into a linear motion in the orthogonal plane, thus generating 3D motion in the true sense. This will help in developing µ-robots, which will use wheels for locomotion (µ-car!). This may also open new avenues for optical MEMS, especially in 3D beam steering.

Bibliography:

[1] Ebefors, T. et. al., "3D micromachined devices based on polyimide joint technology", *Proceedings of the SPIE - The International Society for Optical Engineering,* Vol. 3892, SPIE-Int. Soc. Opt. Eng 1999. pp. 118-32.

[2] E. H. Klaassen et al, "Silicon fusion bonding and deep reactive ion etching: A new technology for microstructures", *Sensors and Actuators A: Physical,* Vol. 52, March 1996, pp. 132-139.

[3] S. Rodgers et. al, "Microelectromechanical Systems-on-a-Chip in a 5-Level Surface Micromachine Technology", *2nd International Conference on Engineering Design and Automation,* Maui, Hawaii, August 9-12, 1998.

[4] J. J. Sniegowski et. al., "IC-Compatible Polysilicon Surface Micromachining", *Annual. Rev. Material Science,* 2000. Vol. 30, pp. 299-333.

[5] M. P. de Boer et. al., "A small area in-situ MEMS test structure to measure fracture strength by electrostatic probing", *SPIE Proceedings, Materials and Device Characterization in Micromachining*, *v. 3875,* CA Sept. 1999.

[6] J. J. Sniegowski et. al, "Monolithic Geared-Mechanisms Driven by a Polysilicon Surface-micromachined On-Chip Electrostatic Microengine", *Solid-State Sensor and Actuator Workshop,* Hilton Head Is., South Carolina, June 2-6, 1996, pp. 178-182.

[7] J. J. Sniegowski et. al., "Surface Micro machined Microengine" *Sensors and Actuators A,* 1995, Vol. 48, pp. 203-214.